HHS Public Access

Author manuscript

Science. Author manuscript; available in PMC 2017 August 02.

Published in final edited form as:

Science. 2016 October 28; 354(6311): 481–484. doi:10.1126/science.aaf6284.

Aerobic glycolysis promotes T helper 1 cell differentiation through an epigenetic mechanism

Min Peng[1,*], **Na Yin**[1,*], **Sagar Chhangawala**[2,3], **Ke Xu**[1,4], **Christina S. Leslie**[2], and **Ming O. Li**[1,†]

[1]Immunology Program, Memorial Sloan Kettering Cancer Center, New York, NY 10065, USA

[2]Computational Biology Program, Memorial Sloan Kettering Cancer Center, New York, NY 10065, USA

[3]Physiology Biophysics and Systems Biology Graduate Program, Weill Cornell Graduate School of Medical Sciences, Cornell University, New York, NY 10065, USA

[4]Immunology and Microbial Pathogenesis Graduate Program, Weill Cornell Graduate School of Medical Sciences, Cornell University, New York, NY 10065, USA

Abstract

Aerobic glycolysis (the Warburg effect) is a metabolic hallmark of activated T cells, and has been implicated in augmenting effector T cell responses including expression of the pro-inflammatory cytokine interferon (IFN)-γ via 3′ untranslated region (3′UTR)-mediated mechanisms. Here we show that lactate dehydrogenase A (LDHA) is induced in activated T cells to support aerobic glycolysis, but promotes IFN-γ expression independently of its 3′UTR. Instead, LDHA maintains high levels of acetyl-CoA to enhance histone acetylation and transcription of *Ifng*. Ablation of LDHA in T cells protects mice from immunopathology triggered by excessive IFN-γ expression or deficiency of regulatory T cells. These findings reveal an epigenetic mechanism by which aerobic glycolysis promotes effector T cell differentiation, and suggest that LDHA may be targeted therapeutically in autoinflammtory diseases.

T cell activation and differentiation is associated with metabolic rewiring (1–4). A metabolic hallmark of activated T cells is aerobic glycolysis (5), the conversion of glucose to lactate in the presence of oxygen, but its physiopathological functions remain incompletely understood (6–8). As the major carbon source, glucose plays important roles in T cell development, proliferation and function (9–15). However, the specific contribution of aerobic glycolysis to T cell responses has not been well defined. Using galactose as a sugar source, aerobic glycolysis was proposed to support IFN-γ expression through 3′UTR-mediated mechanisms (12). Although galactose is metabolized at a slower rate than glucose via the Leloir pathway, both sugars are converted to lactate (16), rendering the galactose system unable to model aerobic glycolysis deficiency in a definitive manner.

†To whom correspondence should be addressed: Dr. Ming O. Li, Immunology Program, Memorial Sloan Kettering Cancer Center, 1275 York Avenue, New York, NY 10065, Phone: (646)-888-2371, Fax: (646)-422-0502, lim@mskcc.org.
*These authors contributed equally to this work.

By converting pyruvate to lactate with regeneration of nicotinamide adenine dinucleotide (NAD^+) (17), lactate dehydrogenase (LDH) defines the biochemical reaction of aerobic glycolysis. LDHA and LDHB form five tetrameric LDH isoenzymes (A_4B_0, A_3B_1, A_2B_2, A_1B_3, and A_0B_4) with distinct kinetic properties (17). In a zymography assay, activated $CD4^+$ T cells manifested LDH activity predominantly in the form of A_4B_0, similar to that of muscle tissues (Fig. S1A). Consistently, LDHA, but not LDHB, was induced upon T cell activation (Fig. S1B), likely due to HIF-1α- and c-Myc-induced transcription of *Ldha* (10, 11).

To study the definitive function of aerobic glycolysis, we deleted LDHA specifically in T cells ($CD4^{Cre}$*Ldha*$^{fl/fl}$, designated as knock-out, KO) (fig. S1B) (18). Compared to activated wild-type (WT) $CD4^+$ T cells, KO T cells barely produced lactate (Fig. 1A). Furthermore, glucose consumption in KO T cells was reduced to ~ 30% WT levels (Fig. 1B), in line with a critical role for LDHA in sustaining aerobic glycolysis through regeneration of NAD^+ consumed at the glyceraldehyde-3-phosphate dehydrogenase (GAPDH) step of glycolysis (17). Consistent with low Glut1 (13) and LDHA expression (fig. S1B), naïve $CD4^+$ T cells showed little activity of glucose metabolism with negligible glucose-induced extracellular acidification rate (ECAR) or oxygen consumption rate (OCR) (Fig. 1, C and D). Upon activation, ECAR was increased in WT $CD4^+$ T cells, which was largely diminished in KO T cells (Fig. 1, C, E and F). In contrast, both basal and maximal OCR were elevated in KO T cells (Fig. 1, D, G and H).

^{13}C-isotope labeled glucose ($^{13}C_6$-glucose) tracing experiments showed that glycolysis was slowed down at the GAPDH step in KO T cells (fig. S2). However, ^{13}C-labelled citrate was increased in the absence of LDHA (fig. S2). In particular, doubly (m+2) and quadruply (m +4) ^{13}C-labeled citrate, readouts of tricarboxylic acid (TCA) cycle activity through the first and second turns, respectively, were much increased in KO T cells (fig. S2), in line with enhanced OCR (Fig. 1, D, G and H). Together, these findings reveal that glucose metabolism in activated $CD4^+$ T cells is shifted from aerobic glycolysis towards oxidative phosphorylation in the absence of LDHA (Fig. 1I).

LDHA deficiency did not affect thymic development of conventional or regulatory T (Treg) cells (fig. S3), or T cell homeostasis in peripheral (fig. S4). LDHA deficiency also did not alter expression of activation markers, size or survival of activated $CD4^+$ T cells (fig. S5, A – D), while proliferation was slightly delayed (fig. S5E). These phenotypes were distinct from those of Glut1-deficient T cells (13), suggesting that general glucose metabolism, but not aerobic glycolysis, is required for T cell development and homeostasis.

Glycolysis promotes expression of effector molecules including the type 1 cytokine IFN-γ (9, 12–15). Indeed, LDHA deficiency led to diminished IFN-γ expression in T cells differentiated under T helper 1 (Th1) conditions (Fig. 2A and 2B). A recent study proposed that aerobic glycolysis enhanced IFN-γ production by sequestering GAPDH away from binding to the *Ifng* 3′UTR thereby enhancing IFN-γ translation (12). To determine whether such regulation accounted for reduced IFN-γ expression in KO T cells, we used a green florescent protein (GFP) reporter in which the GFP open reading frame was fused to the 3′UTR of *Ifng* or *Gapdh*, with the latter not known to repress mRNA translation (19). As

previously reported (19), GFP expression controlled by the *Ifng* 3′UTR showed decreased mean fluorescence intensity compared to that regulated by the *Gapdh* 3′UTR in WT T cells (Fig. 2, C – E). Surprisingly, GFP expression under the control of *Ifng* 3′UTR was diminished to a similar extent in KO T cells (Fig. 2, C – E), suggesting that *Ifng* 3′UTR is insufficient to mediate aerobic glycolysis regulation of IFN-γ expression.

To explore the definitive function of 3′UTR in LDHA control of IFN-γ expression, we used an *Ifng* reporter allele *Yeti* (Yellow-enhanced transcript for IFN-γ) (20), in which the *Ifng* 3′UTR was replaced by 3′UTR of the bovine growth hormone (*BGH*) gene (Fig. 2F). We found that expression of both IFN-γ and yellow fluorescent protein (YFP) driven by the internal ribosome entry site (IRES) element in the reporter allele were proportionally reduced in the absence of LDHA (Fig. 2, G and H), demonstrating that *Ifng* 3′UTR is not required for LDHA control of IFN-γ expression.

To determine whether reduced IFN-γ production in KO T cells was caused by diminished transcription, we performed RNA sequencing experiments. 363 transcripts were differentially expressed between WT and KO Th1 cells, among which 220 transcripts including *Ifng* were downregulated in KO T cells (fig. S6A, S7A and table S1). IFN-γ transcription in Th1 cells is induced by T-bet (21). However, T-bet expression was not affected in KO T cells (fig. S7, B and C), suggesting that LDHA promotes IFN-γ expression via T-bet-independent mechanisms.

Glucose metabolism is implicated in the control of gene expression through epigenetic mechanisms including histone acetylation (7, 22). Chromatin immunoprecipitation-sequencing (ChIP-seq) analysis of histone H3 acetylation at the lysine 9 residue (H3K9Ac), a histone mark associated with active transcription, showed that the differentially expressed genes between WT and KO Th1 cells had varying levels of H3K9Ac (fig. S6B and table S2, S3), which encoded proteins involved in signal transduction, transcription, metabolism and effector functions (fig. S6C). Notably, 86% downregulated transcripts including *Ifng* had decreased H3K9Ac in KO T cells (fig. S6B and table S3), suggesting that LDHA may promote IFN-γ expression by modulating histone acetylation.

Compared to the constitutively active *Cd3e* locus, diminished H3K9Ac was observed in *Ifng* promoter, gene body and the conserved noncoding sequence 22 kilobase pairs upstream of *Ifng* (CNS-22) in KO T cells (Fig. 3, A and B). Acetylation of histone H3 at lysine 27 (H3K27Ac) was also reduced, while total histone H3 was comparable (fig. S8, A and B). Importantly, diminished histone acetylation was associated with reduced RNA polymerse II (PolII) recruitment to the *Ifng* locus in KO T cells (fig. S8C). Histone acetylation requires acetyl coenzyme A (acetyl-CoA) as a substrate with glucose being a critical source. Considering enhanced TCA cycle activity in KO T cells (Fig. 1 and fig. S2), we hypothesized that in the absence of LDHA, less citrate would be exported from the mitochondria for acetyl-CoA regeneration. Indeed, cytosolic acetyl-CoA was decreased in LDHA-deficient Th1 cells (Fig. 3C).

To determine whether reduced cytosolic acetyl-CoA was sufficient to repress IFN-γ expression, we inhibited ATP-citrate lyase (ACL), the enzyme converting citrate to acetyl-

CoA, and found that IFN-γ expression was diminished in WT T cells (fig. S9, A – D). Acetyl-CoA can be generated from acetate by acetyl-CoA synthetase independent of citrate (23). Acetate supplementation augmented acetyl-CoA production (fig. S9E), and corrected IFN-γ expression in KO T cells (Fig. 3, D and E) without affecting T-bet expression (fig. S9F). Instead, enhanced IFN-γ production was associated with normalization of H3K9Ac in *Ifng* promoter and enhancer regions (Fig. 3F). Histone acetylation is a dynamic process controlled by competing activities of histone acetyltransferases (HATs) and histone deacetylases (HDACs) (24). TSA, a HDAC inhibitor, rectified IFN-γ expression in KO T cells without affecting T-bet expression (fig. S9, G and H), which was associated with increased H3K9Ac in the *Ifng* locus (fig. S9I). Collectively, these findings demonstrate that LDHA promotes IFN-γ expression through an epigenetic mechanism of histone acetylation.

In the absence of endogenous 3′UTR, the *Ifng* transcript in *Yeti/Yeti* mice is stable, resulting in sustained IFN-γ production and a lethal autoinflammatory phenotype (25). Indeed, all *Yeti*/*Yeti* mice succumbed to death by 3 weeks of age (Fig. 4A), which was associated with severe liver damage (Fig. 4B and fig. S10A). Deletion of *Ldha* in T cells corrected the liver immunopathology and conferred long-term survival of *Yeti*/*Yeti* mice (Fig. 4, A and B, fig. S10A). LDHA deficiency did not substantially affect the cellularity or activation of *Yeti*/*Yeti* $CD4^+$ T cells (fig. S10, B – E). However, IFN-γ expression in *Yeti*/*Yeti* $CD4^+$ T cells was diminished in the absence of LDHA, while its expression in LDHA-sufficient *Yeti*/*Yeti* NK cells was not affected (Fig. 4, C and D). The correction of a lethal autoinflammatory disease in *Yeti*/*Yeti* mice by T cell-specific deletion of *Ldha* supports that aerobic glycolysis promotes IFN-γ expression in T cells through an epigenetic mechanism of *Ifng* transcription but not via a 3′UTR-dependent mechanism of translation *in vivo*.

To further explore aerobic glycolysis in control of effector T cell responses, we used Scurfy mice with a mutation in the Treg cell lineage *Foxp3* gene (*Foxp3*^{sf}) (26). LDHA deficiency in T cells corrected the Scurfy phenotype and extended life span of *Foxp3*^{sf} mice (fig. S11, A and B), which was associated with reduced inflammation in multiple organs without affecting lymphadenopathy or splenomegaly (fig. S11, C – F). T cell activation and expansion were comparable between *Foxp3*^{sf} and KO *Foxp3*^{sf} mice (fig. S11, G and H), which was in line with our *in vitro* findings (fig. S5, A – E). Nevertheless, $CD4^+$ T cells produced less IFN-γ in the absence of LDHA (fig. S11, I and J), demonstrating a critical role for LDHA-mediated aerobic glycolysis in promoting autoreactive Th1 cell responses.

Our findings do not support a translational mechanism of aerobic glycolysis in IFN-γ production (12), as LDHA promotes IFN-γ expression independent of its 3′UTR. Previous studies have shown that utilization of glycolytic intermediates for biosynthesis accounts for a small fraction (~ 7%) of the glucose consumed in activated T cells (27), while aerobic glycolysis produces the majority (~ 60%) of ATP (28). Hence, LDHA-mediated aerobic glycolysis may primarily relieve the burden of mitochondria as an energy house to ‘burn’ carbons to generate ATP. As a result, more citrate can be exported out of mitochondria to generate acetyl-CoA and promote histone acetylation in selected gene loci (fig. S12). LDHA inhibitors are being developed to target tumor cell metabolism (29). Our data suggest that LDHA inhibitors could be immunosuppressive, and thus may complicate their applications in cancer. Instead, LDHA inhibitors, as well as inhibitors targeting other enzymes involved

in acetyl-CoA metabolism including ACL, may be useful in treatment of autoimmune diseases and transplant rejection.

Supplementary Material

Refer to Web version on PubMed Central for supplementary material.

Acknowledgments

We thank R. Locksley for the *Yeti* mice, A. Abbas and A. Villarino for the 3′UTR GFP constructs, and J. Cross and J. Ye for help with Seahorse experiments. We also thank the Li laboratory for discussions. The data presented in this manuscript are tabulated in the main paper and in the supplementary materials. This work was supported by the Ludwig Center for Cancer Immunology (M.O.L.), the Functional Genomics Initiative (M.O.L.), a Faculty Scholar grant from the Howard Hughes Medical Institute (M.O.L.), and the Memorial Sloan Kettering Cancer Center Support Grant/Core Grant (P30 CA008748). RNA-seq and ChIP-Seq data are deposited in the Genome Expression Omnibus under accession number GSE86188.

REFERENCES AND NOTES

1. Wang R, Green DR. Metabolic checkpoints in activated T cells. Nat Immunol. 2012; 13:907–915. [PubMed: 22990888]
2. Pearce EL, Poffenberger MC, Chang CH, Jones RG. Fueling immunity: insights into metabolism and lymphocyte function. Science. 2013; 342:1242454. [PubMed: 24115444]
3. MacIver NJ, Michalek RD, Rathmell JC. Metabolic regulation of T lymphocytes. Annu Rev Immunol. 2013; 31:259–283. [PubMed: 23298210]
4. Ganeshan K, Chawla A. Metabolic regulation of immune responses. Annu Rev Immunol. 2014; 32:609–634. [PubMed: 24655299]
5. Frauwirth KA, Riley JL, Harris MH, Parry RV, Rathmell JC, Plas DR, Elstrom RL, June CH, Thompson CB. The CD28 signaling pathway regulates glucose metabolism. Immunity. 2002; 16:769–777. [PubMed: 12121659]
6. Heiden, MGVander, Cantley, LC., Thompson, CB. Understanding the Warburg effect: the metabolic requirements of cell proliferation. Science. 2009; 324:1029–1033. [PubMed: 19460998]
7. Lu C, Thompson CB. Metabolic regulation of epigenetics. Cell Metab. 2012; 16:9–17. [PubMed: 22768835]
8. Liberti MV, Locasale JW. The Warburg Effect: How Does it Benefit Cancer Cells? Trends Biochem Sci. 2016; 41:211–218. [PubMed: 26778478]
9. Cham CM, Gajewski TF. Glucose availability regulates IFN-gamma production and p70S6 kinase activation in CD8(+) effector T cells. J Immunol. 2005; 174:4670–4677. [PubMed: 15814691]
10. Wang RN, Dillon CP, Shi LZ, Milasta S, Carter R, Finkelstein D, McCormick LL, Fitzgerald P, Chi HB, Munger J, Green DR. The Transcription Factor Myc Controls Metabolic Reprogramming upon T Lymphocyte Activation. Immunity. 2011; 35:871–882. [PubMed: 22195744]
11. Shi LZ, Wang R, Huang G, Vogel P, Neale G, Green DR, Chi H. HIF1alpha-dependent glycolytic pathway orchestrates a metabolic checkpoint for the differentiation of TH17 and Treg cells. J Exp Med. 2011; 208:1367–1376. [PubMed: 21708926]
12. Chang CH, Curtis JD, Maggi LB Jr, Faubert B, Villarino AV, O'Sullivan D, Huang SC, van der Windt GJ, Blagih J, Qiu J, Weber JD, Pearce EJ, Jones RG, Pearce EL. Posttranscriptional control of T cell effector function by aerobic glycolysis. Cell. 2013; 153:1239–1251. [PubMed: 23746840]
13. Macintyre AN, Gerriets VA, Nichols AG, Michalek RD, Rudolph MC, Deoliveira D, Anderson SM, Abel ED, Chen BJ, Hale LP, Rathmell JC. The Glucose Transporter Glut1 Is Selectively Essential for CD4 T Cell Activation and Effector Function. Cell Metabolism. 2014; 20:61–72. [PubMed: 24930970]
14. Blagih J, Coulombe F, Vincent EE, Dupuy F, Galicia-Vazquez G, Yurchenko E, Raissi TC, van der Windt GJ, Viollet B, Pearce EL, Pelletier J, Piccirillo CA, Krawczyk CM, Divangahi M, Jones RG.

The energy sensor AMPK regulates T cell metabolic adaptation and effector responses in vivo. Immunity. 2015; 42:41–54. [PubMed: 25607458]

15. Ho PC, Bihuniak JD, Macintyre AN, Staron M, Liu XJ, Amezquita R, Tsui YC, Cui GL, Micevic G, Perales JC, Kleinstein SH, Abel ED, Insogna KL, Feske S, Locasale JW, Bosenberg MW, Rathmell JC, Kaech SM. Phosphoenolpyruvate Is a Metabolic Checkpoint of Anti-tumor T Cell Responses. Cell. 2015; 162:1217–1228. [PubMed: 26321681]
16. Bustamante E, Pedersen PL. High aerobic glycolysis of rat hepatoma cells in culture: role of mitochondrial hexokinase. Proc Natl Acad Sci U S A. 1977; 74:3735–3739. [PubMed: 198801]
17. JJ L, HOLBROOK A, STEINDEL SJ, ROSSMANN MG. 4 Lactate Dehydrogenase. The Enzymes. 1975; 11:191–292.
18. See Materials and Methods in Supplementary Materials avaible on line.
19. Villarino AV, Katzman SD, Gallo E, Miller O, Jiang S, McManus MT, Abbas AK. Posttranscriptional silencing of effector cytokine mRNA underlies the anergic phenotype of self-reactive T cells. Immunity. 2011; 34:50–60. [PubMed: 21236706]
20. Stetson DB, Mohrs M, Reinhardt RL, Baron JL, Wang ZE, Gapin L, Kronenberg M, Locksley RM. Constitutive cytokine mRNAs mark natural killer (NK) and NK T cells poised for rapid effector function. J Exp Med. 2003; 198:1069–1076. [PubMed: 14530376]
21. Szabo SJ, Kim ST, Costa GL, Zhang X, Fathman CG, Glimcher LH. A novel transcription factor, T-bet, directs Th1 lineage commitment. Cell. 2000; 100:655–669. [PubMed: 10761931]
22. Wellen KE, Hatzivassiliou G, Sachdeva UM, Bui TV, Cross JR, Thompson CB. ATP-citrate lyase links cellular metabolism to histone acetylation. Science. 2009; 324:1076–1080. [PubMed: 19461003]
23. Luong A, Hannah VC, Brown MS, Goldstein JL. Molecular characterization of human acetyl-CoA synthetase, an enzyme regulated by sterol regulatory element-binding proteins. J Biol Chem. 2000; 275:26458–26466. [PubMed: 10843999]
24. Verdin E, Ott M. 50 years of protein acetylation: from gene regulation to epigenetics, metabolism and beyond. Nat Rev Mol Cell Biol. 2015; 16:258–264. [PubMed: 25549891]
25. Reinhardt RL, Liang HE, Bao K, Price AE, Mohrs M, Kelly BL, Locksley RM. A novel model for IFN-gamma-mediated autoinflammatory syndromes. J Immunol. 2015; 194:2358–2368. [PubMed: 25637019]
26. Brunkow ME, Jeffery EW, Hjerrild KA, Paeper B, Clark LB, Yasayko SA, Wilkinson JE, Galas D, Ziegler SF, Ramsdell F. Disruption of a new forkhead/winged-helix protein, scurfin, results in the fatal lymphoproliferative disorder of the scurfy mouse. Nat Genet. 2001; 27:68–73. [PubMed: 11138001]
27. Hume DA, Radik JL, Ferber E, Weidemann MJ. Aerobic Glycolysis and Lymphocyte-Transformation. Biochem J. 1978; 174:703–709. [PubMed: 310305]
28. Guppy M, Greiner E, Brand K. The Role of the Crabtree Effect and an Endogenous Fuel in the Energy-Metabolism of Resting and Proliferating Thymocytes. Eur J Biochem. 1993; 212:95–99. [PubMed: 8444168]
29. Augoff K, Hryniewicz-Jankowska A, Tabola R. Lactate dehydrogenase 5: An old friend and a new hope in the war on cancer. Cancer Lett. 2015; 358:1–7. [PubMed: 25528630]
30. Dobin A, Davis CA, Schlesinger F, Drenkow J, Zaleski C, Jha S, Batut P, Chaisson M, Gingeras TR. STAR: ultrafast universal RNA-seq aligner. Bioinformatics. 2013; 29:15–21. [PubMed: 23104886]
31. Anders S, Pyl PT, Huber W. HTSeq-a Python framework to work with high-throughput sequencing data. Bioinformatics. 2015; 31:166–169. [PubMed: 25260700]
32. Love MI, Huber W, Anders S. Moderated estimation of fold change and dispersion for RNA-seq data with DESeq2. Genome Biol. 2014; 15
33. Subramanian A, Tamayo P, Mootha VK, Mukherjee S, Ebert BL, Gillette MA, Paulovich A, Pomeroy SL, Golub TR, Lander ES, Mesirov JP. Gene set enrichment analysis: a knowledge-based approach for interpreting genome-wide expression profiles. Proc Natl Acad Sci U S A. 2005; 102:15545–15550. [PubMed: 16199517]
34. Bolger AM, Lohse M, Usadel B. Trimmomatic: a flexible trimmer for Illumina sequence data. Bioinformatics. 2014; 30:2114–2120. [PubMed: 24695404]

35. Langmead B, Salzberg SL. Fast gapped-read alignment with Bowtie 2. Nat Methods. 2012; 9:357–359. [PubMed: 22388286]

36. Zhang Y, Liu T, Meyer CA, Eeckhoute J, Johnson DS, Bernstein BE, Nusbaum C, Myers RM, Brown M, Li W, Liu XS. Model-based analysis of ChIP-Seq (MACS). Genome Biol. 2008; 9:R137. [PubMed: 18798982]

37. Li QH, Brown JB, Huang HY, Bickel PJ. Measuring Reproducibility of High-Throughput Experiments. Ann Appl Stat. 2011; 5:1752–1779.

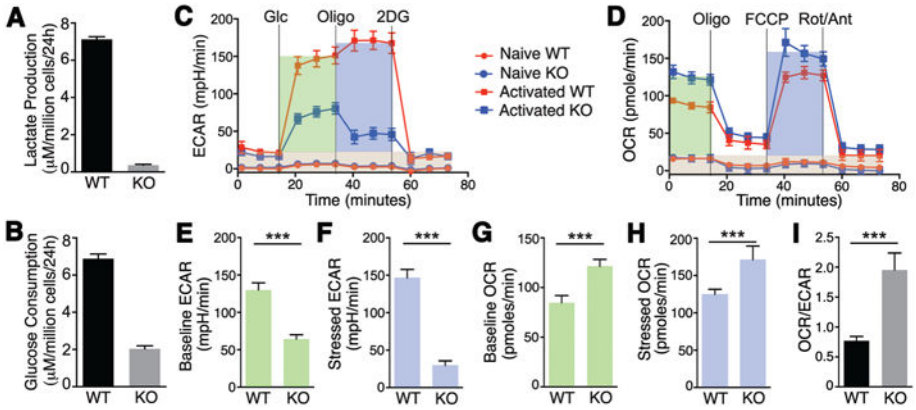

Fig. 1. LDHA dictates aerobic glycolysis in activated CD4$^+$ T cells

(**A** and **B**) Naïve CD4$^+$ T cells isolated from wild-type (WT) or CD4^{Cre}*Ldha*$^{fl/fl}$ (KO) mice were stimulated with anti-CD3 and anti-CD28 in the presence of IL-2 for 2 days. Cells were replenished with fresh medium, which was harvested 24 h later. Lactate production (**A**) and glucose consumption (**B**) were determined with triplicates. (**C** – **I**) Naïve WT or KO CD4$^+$ T cells were stimulated as in (**A**). Extracellular acidification rate (ECAR) and oxygen consumption rate (OCR) were measured with a glycolysis stress test kit (**C**, **E** and **F**) or a Mito stress test kit (**D, G** – **I**). Baseline ECAR (**E**) and stressed ECAR (**F**) of activated CD4$^+$ T cells were calculated according to (**C**). Baseline OCR (**G**), stressed OCR (**H**) and baseline OCR/ECAR (**I**) were calculated according to (**D**). Statistics (**E** – **I**) were from one of two independent experiments each with 8 biological replicates (n = 8), data represent mean ± SD, two-tailed unpaired *t*-test, ***P ≤ 0.001.

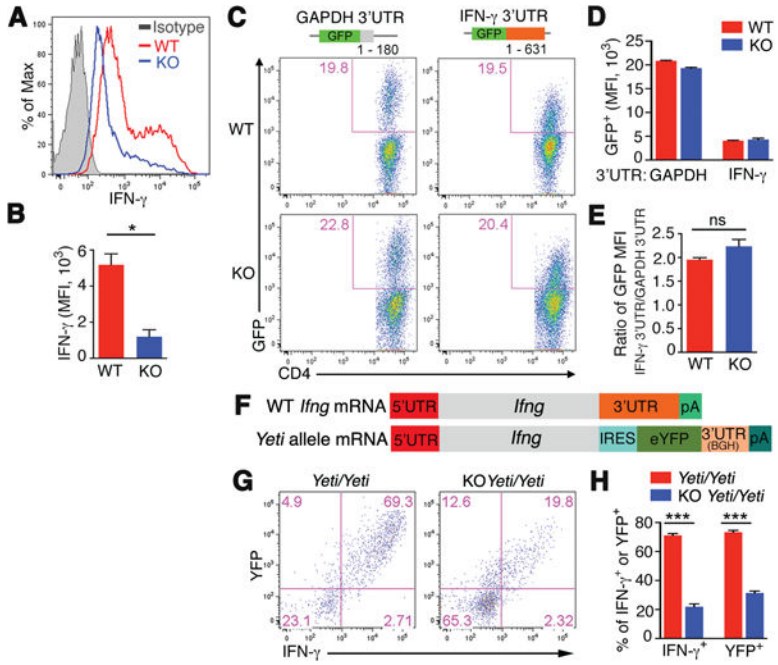

Fig. 2. LDHA regulates IFN-γ expression independent of its 3′UTR

(**A** and **B**) Naïve wild-type (WT) or CD4^{Cre}*Ldha*$^{fl/fl}$ (KO) CD4^{+} T cells were differentiated under Th1 conditions for 3 days, and restimulated with phorbol myristate acetate (PMA) and ionomycin for 4 h. IFN-γ expression was determined by intracellular staining. Representative plots (**A**) and mean fluorescence intensity (MFI) (**B**) are shown. (**C – E**) Naïve WT or KO CD4^{+} T cells were activated for 2 days and transduced with green fluorescent protein (GFP) constructs fused with the 3′ untranslated region (3′UTR) of the *Ifng* or *Gapdh* gene. GFP expression was measured 48 h after transduction. Representative plots (**C**) and MFI of GFP in GFP^{+} cells are shown (**D**). (**E**) MFI of GFP from IFN-γ 3′UTR was normalized to that of GAPDH 3′UTR control. (**F**) A diagram of IFN-γ mRNA expressed from the WT *Ifng* or *Yeti* allele. (**G** and **H**) Naïve CD4^{+} T cells from *Yeti*/*Yeti* or KO *Yeti*/*Yeti* mice were differentiated as in (**A**). The expression of IFN-γ and eYFP were determined by flow cytometry. Representative plots and respective statistic analysis are shown in (**G**) and (**H**). Statistics (**B, E and H**) were from one of two independent experiments each with 3 biological replicates (n = 3), data represent mean ± SD, two-tailed unpaired *t*-test, *P ≤ 0.05; ***P ≤ 0.001; ns, not significant.

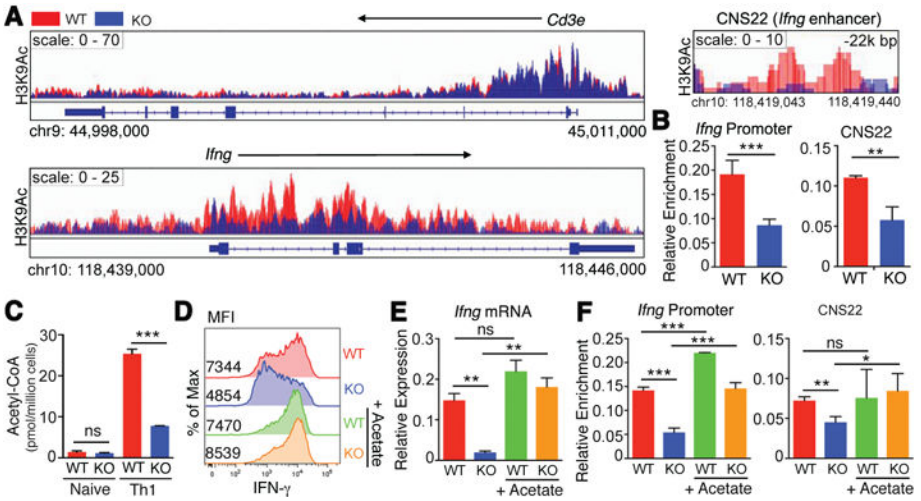

Fig. 3. LDHA promotes IFN-γ expression through an epigenetic mechanism

(**A**) Representative H3K9 acetylation (H3K9Ac) peaks at the *Cd3e* or *Ifng* promoter and enhancer (CNS22) regions from one of two ChIP-Seq experiments are shown. (**B**) H3K9Ac at the *Ifng* promoter and CNS22 enhancer regions in WT or KO Th1 cells were assessed by ChIP-qPCR. Enrichment was normalized to H3K9Ac at the *Cd3e* promoter region. (**C**) Naïve WT or KO $CD4^+$ T cells were differentiated under Th1 conditions, and acetyl-CoA levels were measured by an acetyl-CoA assay kit. (**D** and **E**) Naïve WT or KO $CD4^+$ T cells were differentiated under Th1 conditions for 3 days, and either left untreated or supplemented with 20 mM sodium acetate for another 24 h. Cells were subsequently restimulated with phorbol myristate acetate (PMA) and ionomycin for 4 h. The expression of IFN-γ protein (**D**) and mRNA (**E**) were determined by flow cytometry and qPCR, respectively. mRNA level of IFN-γ was normalized to that of β-Actin. MFIs of IFN-γ are shown in (**D**). (**F**) T cells were cultured as in (**D**), and H3K9Ac at the *Ifng* promoter and CNS22 enhancer regions were assessed by ChIP-qPCR. Enrichment was normalized to H3K9Ac at the *Cd3e* promoter region. Statistics (**B, C, E and F**) were from one of three independent experiments each with 3 biological replicates (n = 3), data represent mean ± SD, two-tailed unpaired *t*-test, *P ≤ 0.05; **P ≤ 0.01; ***P ≤ 0.001; ns, not significant.

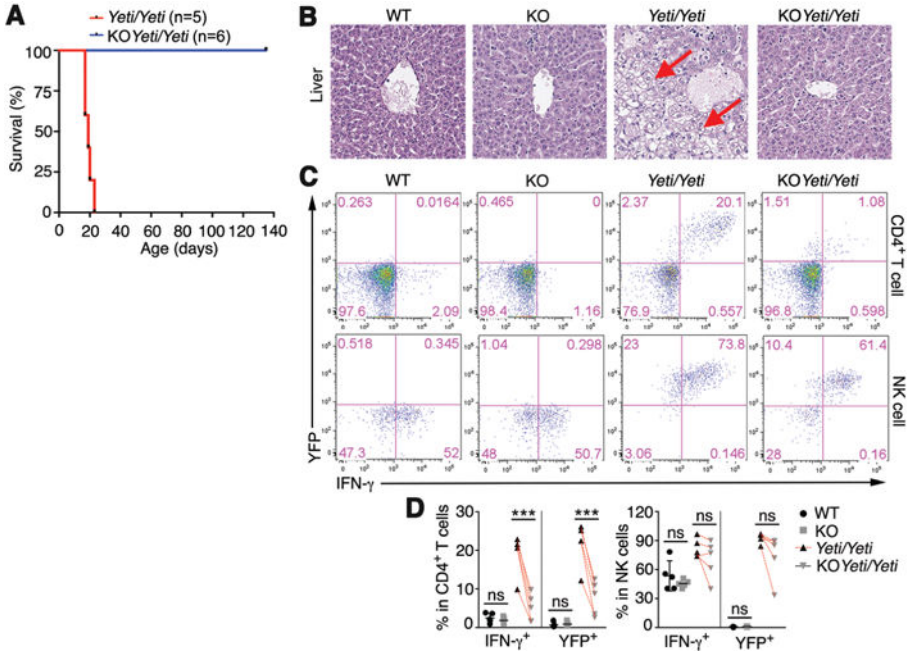

Fig. 4. LDHA deficiency in T cells protects *Yeti/Yeti* mice from a lethal autoinflammatory disease

(**A**) The survival curve of *Yeti/Yeti* (n = 5) and $CD4^{Cre}Ldha^{fl/fl}$ *Yeti/Yeti* (KO *Yeti/Yeti*) mice (n = 6). (**B**) Representative haematoxylin and eosin staining of liver sections from wild-type (WT), $CD4^{Cre}Ldha^{fl/fl}$ (KO), *Yeti/Yeti* and KO *Yeti/Yeti* mice. Arrows indicate the necrotic regions. (**C** and **D**) Splenocytes from mice of the indicated genotypes were stimulated with phorbol myristate acetate (PMA) and ionomycin for 4 h. IFN-γ and YFP expression in $CD4^+$ T cells and $NK1.1^+TCR^-$ NK cells were determined by flow cytometry. Representative plots (**C**) and statistics (**D**) are shown, data represent mean ± SD, n = 4 – 5 mice per genotype, two-tailed paired *t*-test, ***P ≤ 0.001; ns, not significant.